Biotechnology and Applied Biochemistry

WILEY

IUBMB

ORIGINAL ARTICLE

A Quartz Tuning Fork-Based Immunosensor for Detection of Kidney Injury Molecule-1: A New Working Electrode for Electrochemical Applications

Şeyma Şentürk Özkan | Mustafa Kemal Sezgintürk

Bioengineering Department, Engineering Faculty, Çanakkale Onsekiz Mart University, Çanakkale, Türkiye

Correspondence: Mustafa Kemal Sezgintürk (msezginturk@hotmail.com)

Received: 11 March 2025 | **Accepted:** 27 December 2025

Keywords: 11-mercaptoundecanoic acid (11-MUA) | immunosensor | kidney injury | kidney injury molecule-1 (KIM-1) | quartz tuning fork (QTF) electrode

ABSTRACT

Kidney injury molecule-1 (KIM-1) is a Type I transmembrane glycoprotein and is a potential biomarker for detecting kidney damage, as its urinary levels fluctuate in cases of acute kidney injury. In this study, an electrochemical immunosensor was developed for the first time using a quartz tuning fork (QTF) working electrode to detect the KIM-1 biomarker. The gold-tipped QTF electrode surface was modified with 11-mercaptoundecanoic acid (11-MUA) to form a self-assembled monolayer (SAM). To construct the biosensor, extensive optimization studies were conducted on the fabrication parameters, followed by characterization and real urine sample testing to evaluate its applicability. Electrochemical impedance spectroscopy (EIS) and cyclic voltammetry (CV) methods were utilized in all electrochemical experiments. Morphological changes on the QTF electrode surface were examined using atomic force microscopy (AFM) and scanning electron microscopy (SEM). The developed electrochemical KIM-1 immunosensor demonstrated highly promising performance, exhibiting an exceptionally wide detection range (0.05–250 fg/mL). Furthermore, the dissociation constant (Kd) of the interaction between KIM-1 and its antibody was successfully calculated using the Hill equation, on the basis of the QTF-based system.

1 | Introduction

The kidney has many functions such as excretion, hormone production, blood pressure regulation, and maintenance of ionic, osmotic, and pH balance, all of which make the kidney essential for physiological homeostasis. Because of these diverse roles, kidney diseases often have systemic consequences, which bring challenges and high costs in their diagnosis and treatment [1]. Investigating biomarkers for the early detection of kidney damage is critical, as treatment can be initiated before a decline in kidney function occurs. For this reason, it is important to have a sensitive, specific, and noninvasive biomarker for the early detection of kidney injury. One of the most promising potential biomarkers is kidney injury molecule-1 (KIM-1) [2]. KIM-1 is a Type I cell membrane glycoprotein that contains a unique six-cysteine immunoglobulin-like domain and a mucin-rich extracellular region, both of which are conserved across species [3]. Also known as HAVcr-1 and TIM-1, KIM-1 is a transmembrane glycoprotein that belongs to the T-cell immunoglobulin and mucin domain family—a group of glycoproteins expressed on immune cells involved in regulating immune responses. KIM-1 differs from other members of this family in that it is expressed not only by immunocompetent cells but also by epithelial cells [4].

KIM-1, a biomarker for the diagnosis of acute kidney injury (AKI), is highly specific for kidney injury due to its detectability in urine. After AKI, an extracellular portion of KIM-1 is excreted into

the urine and can be detected there [5]. The rising incidence of various diseases in recent years, along with the increasing presence of harmful substances affecting living organisms and their devastating consequences, underscores the critical importance of early diagnosis. For this reason, the need for effective diagnostic methods is steadily increasing.

Complex methods, such as enzyme-linked immunosorbent assay (ELISA) [3], the colorimetric Jaffe reaction [6], and high-performance liquid chromatography [7], are commonly used to detect kidney biomarkers. Although these conventional methods are effective, they are often time-consuming, labor-intensive, and expensive and require specialized equipment and expertise. Consequently, there is growing interest in systems that are more advantageous in terms of time, ease of use, and cost.

Biosensors offer a promising alternative thanks to their simplicity, affordability, portability, and rapid response even in complex samples [8].

Quartz tuning forks (QTFs) are widely used as oscillator components due to their stable resonant frequencies. Recently, QTFs have been employed as transducers in (bio)sensing systems, demonstrating the potential to produce highly sensitive and reliable mass sensors [9, 10]. Although the QTF electrode offers many advantages such as high sensitivity, low cost, and ease of multiple modifications, its fragile structure can be considered a disadvantage.

In this study, an Au-tipped QTF electrode was used as the working electrode in the electrochemical biosensor system, leveraging the electrode surface's conductivity. An innovative, sensitive, specific, and affordable electrochemical biosensor was developed for the detection of the KIM-1 biomarker.

2 | Materials and Methods

2.1 | Reagents and Equipment

All chemicals were purchased from Sigma Aldrich (USA). QTF electrodes were obtained from a local technology market (CFS-14532768DZFB, originally produced by Citizen Finedevice Co Ltd.) and used as working electrodes in the conventional three-electrode setup for the electrochemical measurements. Simultaneously, Ag/AgCl and platinum wire served as the reference and counter electrode, respectively. Ultrapure water was obtained from an Elga LC134 system (18.2 MΩ cm). KIM-1 and anti-KIM-1 antibodies were purchased from MyBioSource, San Diego, USA, and both were prepared in pH 7.4 phosphate buffer. All electrochemical experiments were performed using Gamry potentiostat/galvanostat (Reference 600, Gamry Instruments, Warminster, PA, USA), and electrochemical measurements were performed in 5 mM $[Fe(CN)_6]^{3-/4-}$ solution containing 0.1 M KCl as a redox probe. The atomic force microscopy (AFM) and scanning electron microscopy (SEM) measurements were conducted at the Science and Technology Application and Research Center of Çanakkale Onsekiz Mart University (ÇOBİLTUM).

2.2 | Electrochemical Measurements

Electrochemical impedance spectroscopy (EIS) and cyclic voltammetry (CV) measurements were taken to examine the surface characteristics and monitor bonding at each optimization step and at different KIM-1 concentrations. Electrochemical measurements were carried out using the redox probe, which was 5 mM $[Fe(CN)_6]^{3-/4-}$ solution containing 0.1 M KCl. The applied potential for CV measurements was chosen between −0.5 and 0.7 V, with a step size of 10 mV and a sweep rate of 100 mV/s. The formal potential applied in impedance measurements was 0 V, with an alternating current amplitude of 5 mV. Impedance measurements were performed over a frequency range from 50,000 to 0.05 Hz.

2.3 | Design Strategy of KIM-1 Immunosensor

In the immobilization stage, the Au-tipped QTF electrode was first soaked in a 50-μM 11-mercaptoundecanoic acid (11-MUA) solution overnight to form a self-assembled monolayer (SAM) in a 3D-printed special vessel with a volume of 100 μL. Then, the resulting 11-MUA/Au electrode was rinsed with its solvent, ethanol, and then with ultrapure water, respectively, to remove unbound molecules. Electrodes modified with 11-MUA, 0.4 mM *N*-(3-dimethylaminopropyl)-*N*-ethylcarbodiimide hydrochloride (EDC), and 0.1 mM *N*-hydroxysuccinimide (NHS) for activation of the carboxylic acid terminal groups of 11-MUA and to enable covalent interaction with amino groups in the anti-KIM-1 antibody were incubated for 60 min. After creating a suitable surface for antibody immobilization, each electrode was incubated in 10 μL of a 100-pg/mL anti-KIM-1 solution for 45 min. After incubation with the anti-KIM-1 antibody, the electrodes were rinsed with ultrapure water to remove unbound antibody molecules. Finally, the electrodes were incubated in 0.005% BSA for 60 min to block unbound active carboxyl groups and then rinsed again with ultrapure water to remove unbound molecules. The biosensor, whose immobilization phase was completed, was stored at +4°C until the measurement of the KIM-1 antigen was performed. The immobilization steps of the developed KIM-1 immunosensor are shown in Figure 1.

In order to determine the optimal fabrication parameters of the immunosensor developed for KIM-1 determination, optimization studies were performed for the concentrations of 11-MUA and anti-KIM-1, EDC–NHS incubation time, anti-KIM-1 incubation time, KIM-1 concentration, and KIM-1 incubation time.

3 | Results and Discussion

3.1 | Immobilization Processes of KIM-1 Immunosensor

After each immobilization step of the immunosensor, EIS and CV measurements were performed to monitor changes on the electrode surface. EIS measurements of the immobilization steps of the immunosensor developed for KIM-1 determination are shown in Figure 2A, and CV measurements are shown in Figure 2B.

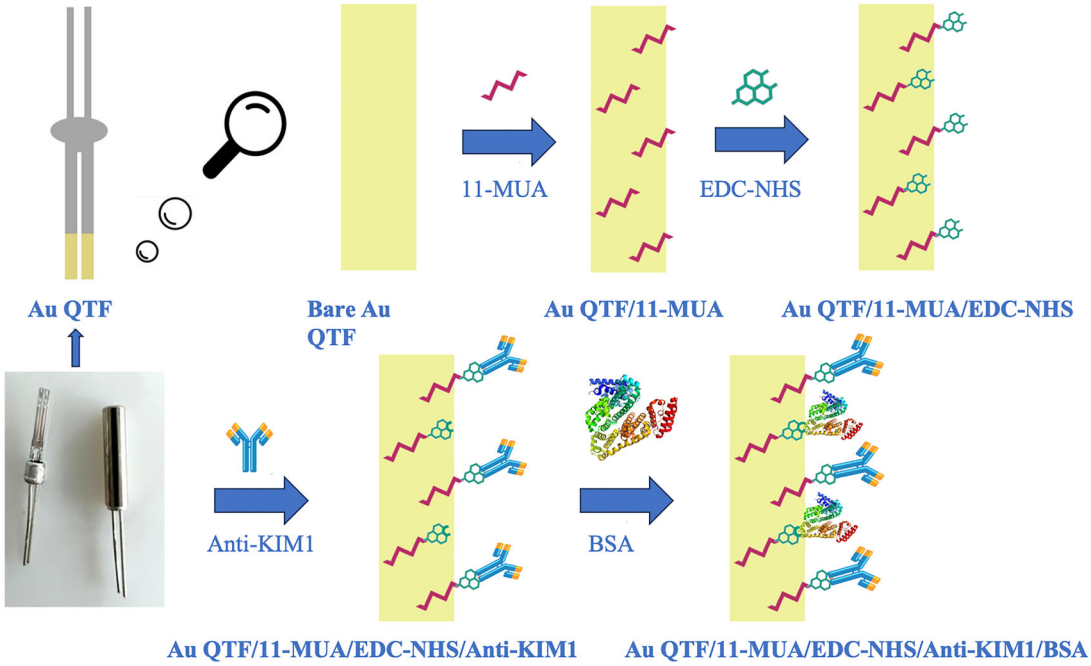

FIGURE 1 | Immobilization steps of the KIM-1 immunosensor. KIM-1, kidney injury molecule-1.

In electrochemical immunosensors, the conductivity properties of the electrode surface usually change after each modification. To monitor these changes, each modification step performed on the electrode surface was examined by CV and EIS. In the first step of immobilization, an SAM layer was formed by attaching 11-MUA with –SH groups to the gold surface of the QTF electrode. As 11-MUA has a long-chain structure and functional negatively charged carboxyl terminals that hinder the diffusion of the redox probe through the electrode surface, as shown in Figure 2A, the R_{ct} value of the 11-MUA-modified electrode surface was quite high; accordingly, the semicircle diameter in the Nyquist diagram was also large. In the characteristic peaks of the cyclic voltammograms obtained with 11-MUA modification (Figure 2B), it was observed that the peak current decreased due to surface insulation. These findings provide evidence of successful SAM layer formation by 11-MUA modification. After 11-MUA modification, the electron transfer rate increased and the electron transfer resistance decreased significantly with the immobilization of EDC–NHS, which acts as a cross-linker to activate the carboxyl groups on the surface, thus reducing the semicircle diameter in the EIS experiments. Similarly, this effect caused an increase in peak currents, as seen in Figure 2B. After the antibody binds to the surface via covalent bonding, the layer formed creates a barrier effect, resulting in insulation and an increase in the semicircle diameter in the Nyquist diagram. In the final immobilization step, the electrode surface was modified with BSA to block unbound active sites and prevent nonspecific interactions after antibody–antigen binding. In this case, the charge transfer resistance increased. Figure 2B shows that the CV results are consistent with the impedance spectra in Figure 2A. Due to the layered insulating layer formed on the surface, the ferri/ferro redox couple is prevented from approaching the surface, and therefore, the anodic and cathodic peak currents decreased. Moreover, to investigate the surface morphological changes occurring during the stepwise fabrication of the developed biosensor, scanning electron microscopy (SEM) and atomic force microscopy (AFM) analyses were carried out. The representative SEM and AFM images corresponding to each preparation stage are presented in the Supplementary Information (Supporting information).

3.2 | The Optimization Steps of KIM-1 Immunosensor

Optimization studies are vital for a biosensor to achieve the best working performance. In the optimization studies, the optimum concentration of 11-mercaptoundodecanoic acid used to form the SAM layer in the preparation of the KIM-1 biosensor was first determined. For this purpose, three different biosensor systems were prepared by forming the SAM layer with 11-MUA solutions at concentrations of 5, 50, and 500 μM. The other fabrication parameters used in the construction of the biosensor were kept constant. According to the measured values, 50 μM was chosen as the most appropriate concentration, as shown in Figure 3A. Then, EDC–NHS chemistry was used to activate the carboxyl ends of 11-MUA [11, 12]. At this stage, three different biosensor systems were prepared using different incubation times of 30, 45, and 60 min, keeping all other concentrations and parameters the same. These experiments revealed that the optimal EDC–NHS incubation time was 45 min, as shown in Figure 3B. At incubation times shorter than 45 min, it was clear that antibody immobilization was insufficient for forming a stable biorecognition layer. It was also observed that the electrode surface was damaged during incubation periods longer than 45 min. To evaluate the effect of antibody concentration on the QTF-based immunosensor, three biosensor systems were prepared using anti-KIM-1 antibody concentrations of 50, 100, and 200 pg/mL (Figure 3C). The experimental results showed that the signals obtained with 50 pg/mL antibody were insufficient, whereas, at 200 pg/mL, the biosensor did not perform as well as expected. Therefore,

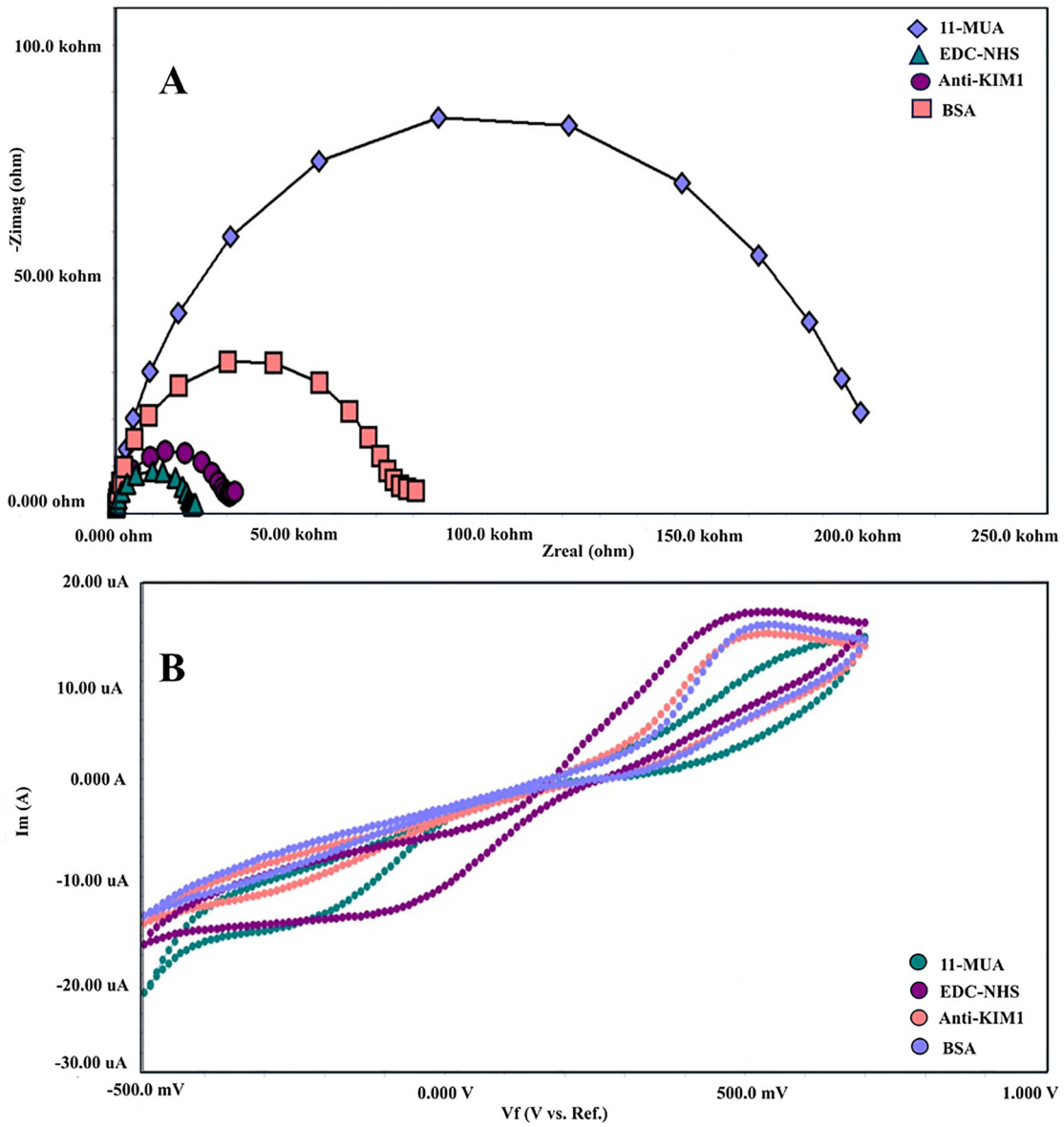

FIGURE 2 | Immobilization processes of KIM-1 immunosensor [(A) EIS spectra and (B) CV voltammograms (electrochemical measurements were carried out using the redox probe, which was 5 mM $[Fe(CN)_6]^{3-/4-}$ solution containing 0.1 M KCl. The applied potential for CV measurements was between −0.5 and 0.7 V, with a step size of 10 mV and a sweep rate of 100 mV/s. The formal potential applied in impedance measurements was 0 V, with an alternating current amplitude of 5 mV. Impedance measurements were performed over a frequency range from 50,000 to 0.05 Hz. KIM-1, kidney injury molecule-1.

100 pg/mL was selected as the optimal antibody concentration, on the basis of the electrochemical signals obtained.

After selecting the antibody concentration, three biosensor systems were prepared with varying antibody incubation times of 30, 45, and 60 min, keeping all other conditions constant. The results clearly showed that 30 min of incubation was insufficient to form a stable biorecognition layer. When the incubation time was increased to 60 min, the electrochemical signals again decreased. This was attributed to the formation of an undesirably thick biorecognition layer with longer incubation. As clearly seen in Figure 3D, the best results were obtained with a 45-min incubation period. For the final optimization study, the effect of KIM-1 incubation time on the immunosensor performance was evaluated by preparing three KIM-1 calibration graphs using incubation periods of 30, 45, and 60 min (Figure 3E). The results were similar to those obtained for antibody incubation time. This suggests that as incubation time increases, the amount of protein on the electrode surface also increases. However, both studies revealed that excessive protein on the surface does not enhance the biosensor response. As a consequence, 45 min was determined to be the most appropriate incubation time.

3.3 | Analytical Properties of KIM-1 Immunosensor

After completing the optimization experiments, critical analyses were conducted to evaluate the analytical performance of the QTF-based KIM-1 immunosensor. As shown in Figure 4A, the

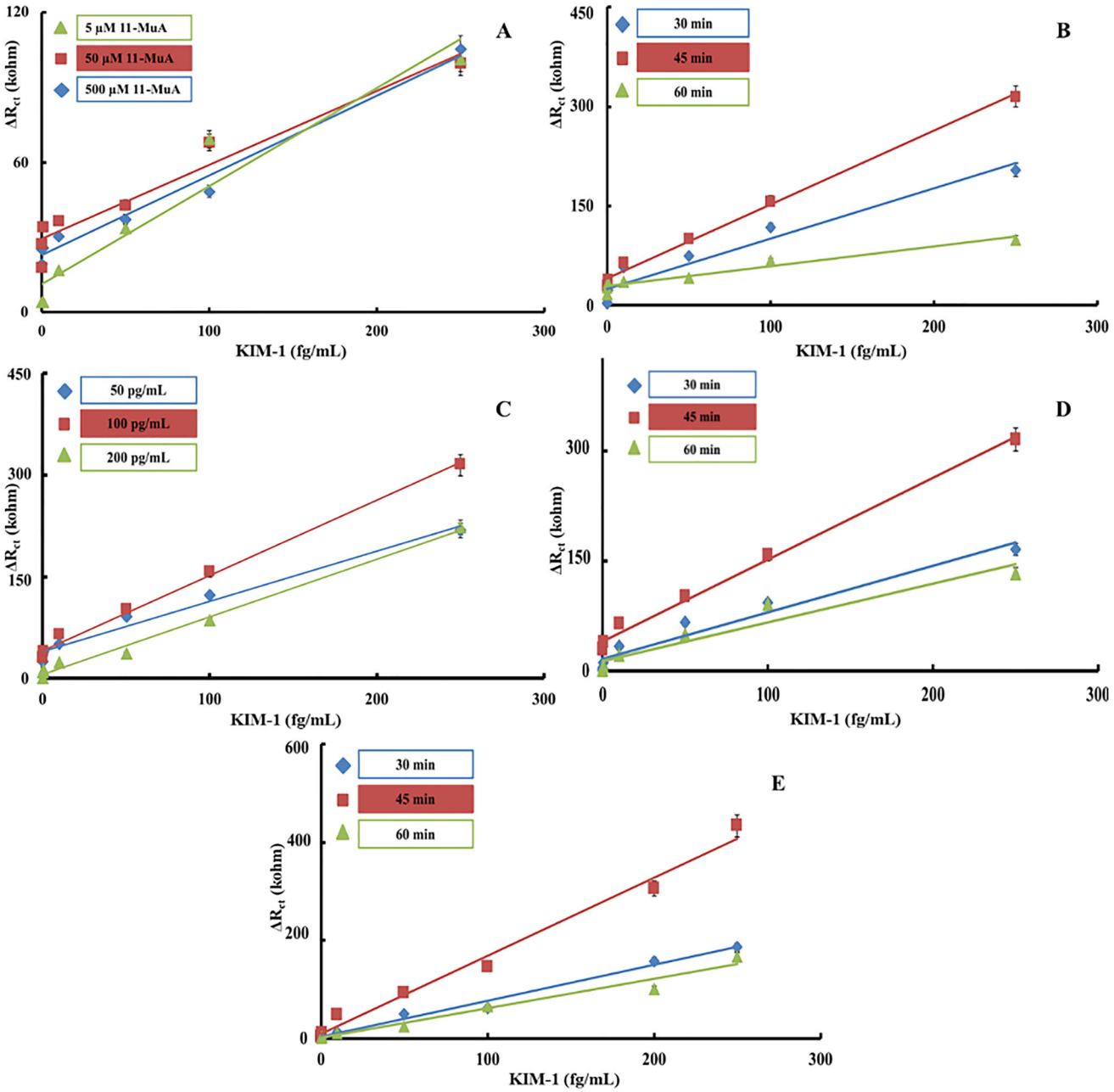

FIGURE 3 | Optimization steps of KIM-1 immunosensor [(A) 11-MUA concentration optimization, (B) EDC–NHS time optimization, (C) anti-KIM-1 concentration optimization, (D) anti-KIM-1 time optimization, (E) KIM-1 concentration optimization, and (F) KIM-1 time optimization]. 11-MUA, 11-mercaptoundecanoic acid; KIM-1, kidney injury molecule-1.

semicircle diameter in the Nyquist plots increased progressively with rising KIM-1 concentrations, indicating that the impedance correspondingly increased with higher KIM-1 levels. Similarly, Figure 4B demonstrates that as the concentration of KIM-1 increased, the accumulation of KIM-1 on the immunosensor surface created an insulating layer, which caused a reduction in the oxidation and reduction peak currents of the redox probe. This observation is consistent with the impedance results from EIS measurements.

Figure 4C presents the calibration curve for the KIM-1 immunosensor, revealing a broad linear detection range from 0.05 to 250 fg/mL. From these data, the limit of detection (LOD) was calculated as 14.9 fg/mL using the formula LOD = $(3 \times \sigma)/S$, and the limit of quantification (LOQ) was determined as 49.5 fg/mL using LOQ = $(10 \times \sigma)/S$, where σ is the standard deviation of the blank and S is the slope of the calibration curve. The regression equation was found to be $y = 1571.2$ [KIM-1] + 10,981, with an excellent correlation coefficient of 0.9987. For impedance-based biosensors, linearity and stability are crucial for reliable measurements. To confirm that the impedance data were free from external disturbances, the Kramers–Kronig transformation was applied [13]. The transformed impedance data perfectly matched the real experimental values, as illustrated in Figure 4D, confirming that the QTF-based biosensor was not influenced by external noise or artifacts. An important aspect of immunosensor

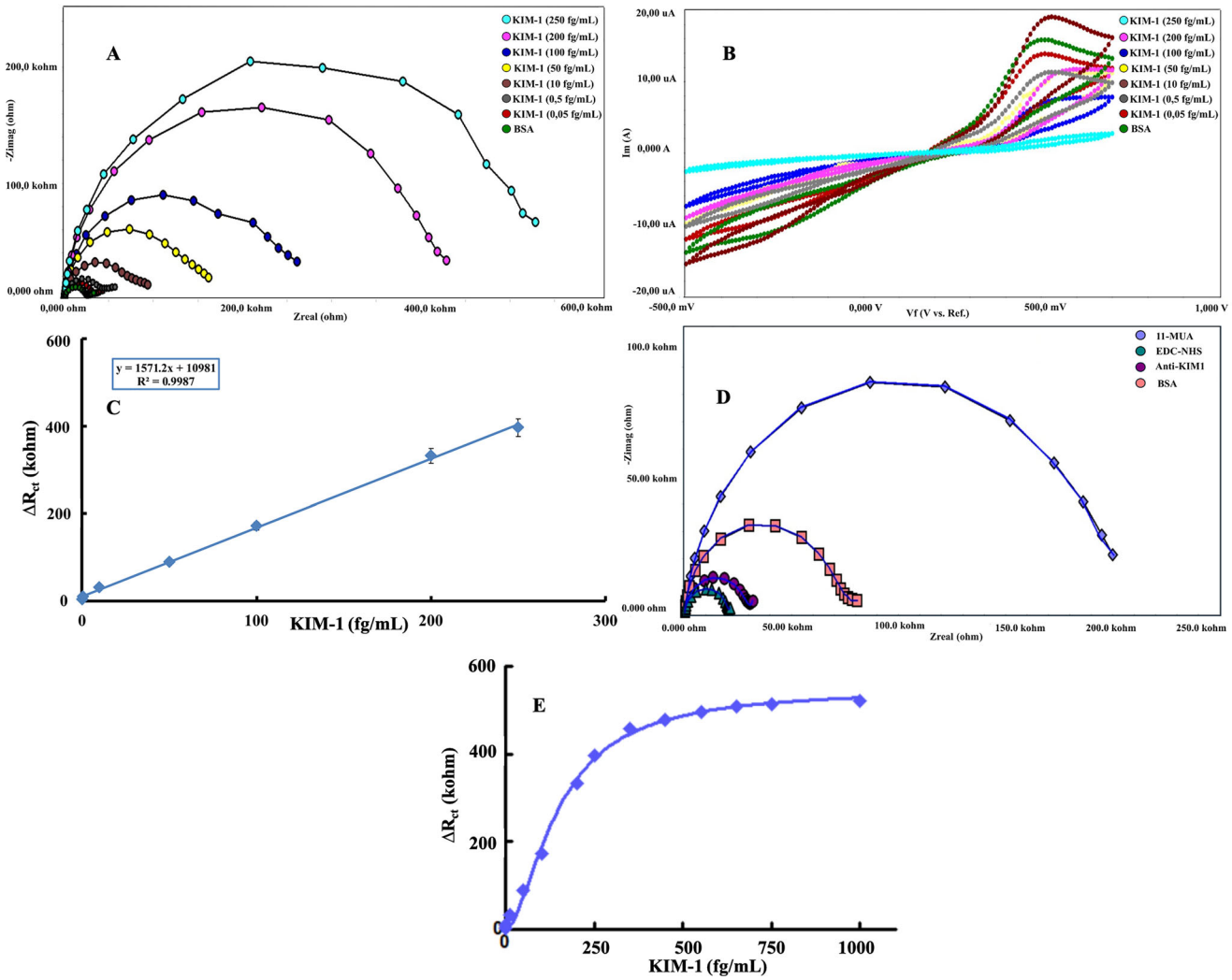

FIGURE 4 | Analytical properties of KIM-1 immunosensor [(A) EIS spectra of the designed immunosensor, (B) CV voltammograms of the immunosensor, (C) calibration curve, (D) Kramers–Kronig transformation, (E) dissociation constant graph]. KIM-1, kidney injury molecule-1.

characterization is the calculation of the dissociation constant (K_d), which provides valuable information about the binding affinity between the immobilized antibody and its antigen [14, 15]. A significant achievement in this study was the determination of the K_d value for the interaction between anti-KIM-1 and KIM-1. For this purpose, KIM-1 concentrations exceeding the previously determined detection range were analyzed. The data were fitted using a nonlinear regression function in GraphPad Prism 5.0 software. The change in charge transfer resistance (ΔR_{ct}) was plotted against KIM-1 concentrations to generate the binding curve, as shown in Figure 4E. The following equation, on the basis of the Hill model, was used to calculate K_d, where ΔR_{ct} values were obtained by subtracting the R_{ct} of BSA from that of KIM-1 ($\Delta R_{ct} = R_{ct}(\text{KIM-1}) - R_{ct}(\text{BSA})$) and plotted against KIM-1 concentration:

$$\Delta R_{ct} = \frac{B_{max}\,[\text{KIM} - 1]^h}{\text{K}^h{}_d + [\text{KIM}{-}1]^h}$$

In this equation, B_{max} represents the maximum biosensor response corresponding to the saturated KIM-1 concentration, K_d is the KIM-1 concentration at which the biosensor signal reaches half of its maximum value, and h is the Hill coefficient reflecting the cooperativity of the binding interaction. The K_d value calculated using this equation was 148 ± 7 fg/mL. Analysis of the binding curve shown in Figure 4E reveals that linearity is lost at KIM-1 concentrations above 250 fg/mL, indicating that the antibody–antigen binding sites become saturated beyond this concentration in the developed immunosensor system. In other words, the selected detection range (0.05–250 fg/mL) effectively captures the dynamic binding behavior and is well-suited for the immunosensor's analytical performance.

Repeatability study is an important characterization to determine whether the developed immunosensor can provide consistent measurements. For this purpose, 20 biosensors were prepared under optimal conditions and measured at the same KIM-1 concentration (50 fg/mL), and their electrochemical signals were analyzed. The mean, standard deviation, and coefficient of variation based on impedance measurements were calculated as 50.18 fg/mL, 0.7 fg/mL, and 1.394%, respectively. A graphical representation of the repeatability study is shown in Figure 5A. As seen in the graph and confirmed by these statistics, the developed immunosensor demonstrated excellent repeatability.

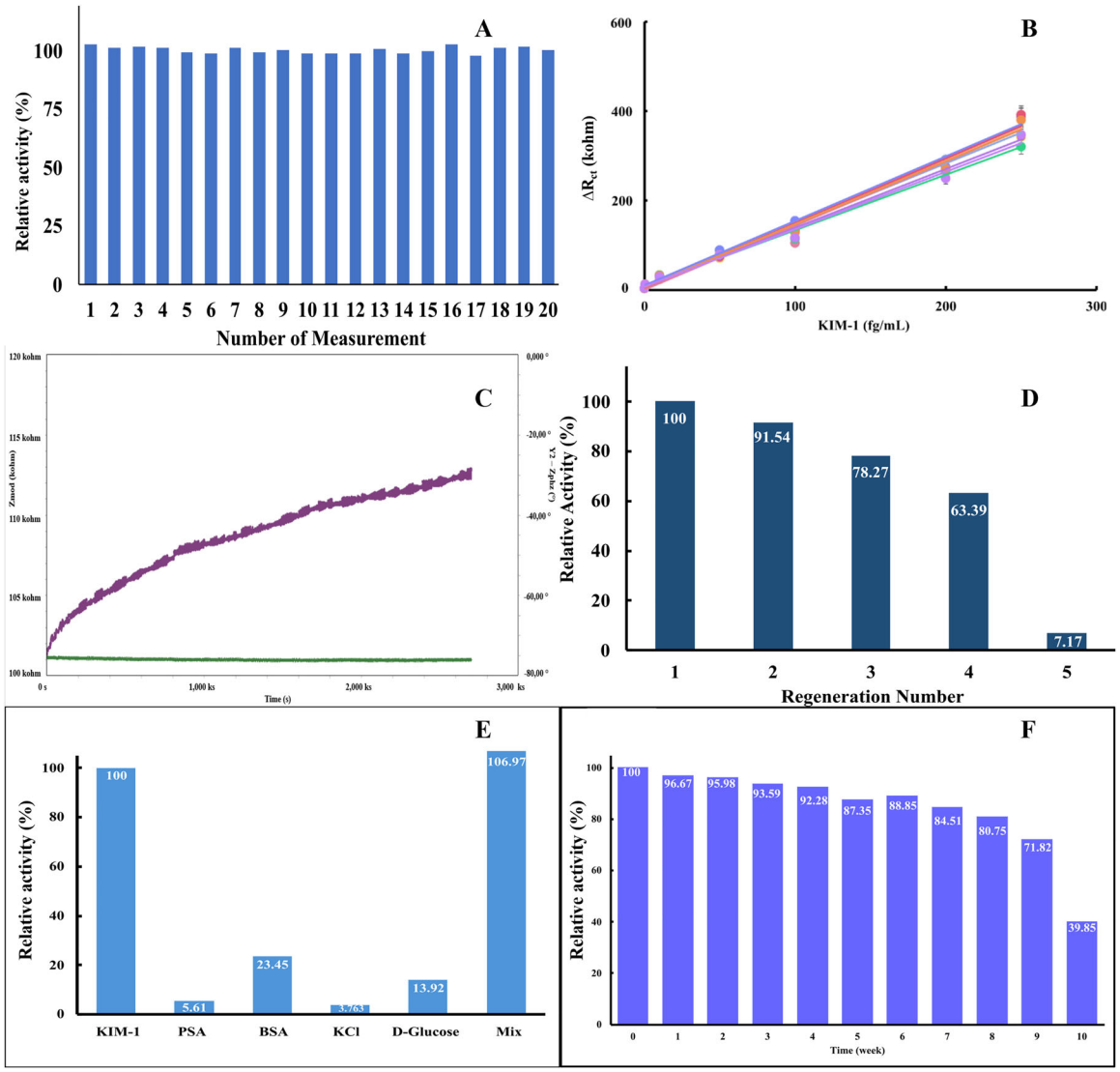

FIGURE 5 | Electrochemical characterization of the biosensor [(A) Repeatability, (B) reproducibility, (C) SFI, (D) regeneration, (E) specificity, and (F) storage life]. KIM-1, kidney injury molecule-1.

A reproducibility study was also conducted to verify that the biosensor is accurate, stable, reliable, and reproducible under the same standard working and fabrication conditions. To evaluate reproducibility, 10 calibration plots for KIM-1 were prepared using disposable immunosensors. The calibration curves obtained are presented in Figure 5B, where it can be observed that all graphs almost completely overlap. On the basis of this reproducibility study, the relative standard deviation (RSD) for the slope was calculated as 5.65%, confirming the high reproducibility of the developed immunosensor system.

Single frequency impedance (SFI) experiments are particularly important for the simultaneous monitoring of antibody–antigen binding. Moreover, this electrochemical method is highly valuable as it easily tracks concurrent molecular interactions [16, 17]. For this reason, the impedance changes during the entire incubation period of the antibody–antigen interaction were monitored at a fixed frequency. The SFI measurements were carried out by using the frequency of 100 Hz. For this purpose the potentiostat was set up at a fixed frequency, such as 100 Hz. The impedance was measured at this fixed frequency as a function of time and phase angle for 45 min. The resulting graph from the SFI study is presented in Figure 5C. As seen in the graph, binding on the immunosensor surface began immediately after the KIM-1 antigen was introduced into the reaction cell, and instantaneous binding continued for the 45 min previously determined during the optimization studies. The green line represents the variation in the phase angle throughout the antibody–antigen interaction.

An important advantage of the developed biosensor is the potential for reuse, which provides an economic benefit compared to disposable devices. To evaluate this, a regeneration study was conducted to determine whether the disposable QTF electrode could be reused multiple times. In this study, the immunosensor with bound KIM-1 was treated with a 0.05% HCl solution for 3 min to disrupt the interaction between anti-KIM-1 and KIM-1. After each acid treatment, the immunosensor was re-incubated with KIM-1 antigen (50 fg/mL), and impedance measurements were recorded. This regeneration cycle was repeated five times; however, after the fifth treatment, the immunosensor showed sig-

nificant degradation. Therefore, the immunosensor system could be effectively regenerated up to four times. The regeneration study results are illustrated in Figure 5D. These findings suggest that although reusability of the disposable biosensor system can offer economic advantages, QTF-based immunosensors appear to have limited suitability for multiple reuses due to structural degradation.

Specificity is one of the most critical characteristics for evaluating a newly developed biosensing system. The antibody, anti-KIM-1, is scientifically expected to bind specifically to its corresponding antigen and not interact with other substances. However, in certain cases, nonspecific interactions can occur. To investigate and clarify this, several proteins and metabolites were tested as potential interferents on the biosensing system. The results are presented in Figure 5E. As observed, the developed immunosensor demonstrated high specificity, showing negligible interference from other substances.

Finally, the storage stability of the biosensor was evaluated. It is well known that a long storage life is a valuable and desirable feature for any biosensor. To assess the impact of storage on the biosensor's performance, multiple biosensors were prepared under identical optimal conditions and stored at +4°C for various durations. At the end of each storage period, each biosensor was incubated in 50 fg/mL KIM-1 antigen, followed by standard measurement procedures. The performance results over time are summarized in Figure 5F. The biosensor retained approximately 92% of its initial activity at the end of the fourth week. However, by the ninth week, a decline in activity of around 28% was observed. At the end of the 10th week, the biosensor's operational efficiency had significantly decreased, indicating a notable loss of functionality.

Current biosensor systems for KIM-1 detection have already been reported in the literature. In 2018, Yang et al. developed a novel electrochemiluminescence (ECL) immunosensor with high luminous efficiency for KIM-1 analysis. An AuNP-modified glassy carbon electrode (GCE) was used as the working electrode. They found that the LOD of the immunosensor, with a detection range of 50 fg/mL–1 ng/mL, was 16.7 fg/mL, demonstrating the high sensitivity of the developed system. This study suggested that such a platform holds great promise for future applications in bioanalysis due to the simplicity, efficiency, and aqueous stability of the dual-enhanced ECL emitter [18].

In 2021, Liu et al. developed a novel enzyme-free electrochemical immunosensor on the basis of a quaternary metallic/nonmetallic PdPtBP alloy mesoporous nanoparticle (MNP)/MXene composite and $CuCl_2$ nanowires (NWs) for KIM-1 detection. A GCE modified with highly conductive $CuCl_2$ NWs and biocompatible AuNPs was used as the working electrode. The immunosensor exhibited a strong linear response in the range of 0.5–100 ng/mL, with an LOD of 86 pg/mL [19]. In 2022, Boyacıoğlu et al. developed a rapid, sandwich-type electrochemical immunosensor for KIM-1 detection, utilizing porous $NiCo_2S_4$@CeO_2 microspheres as a signal amplifier and a covalent organic framework-gold nanoparticle (COF-AuNP) composite as the electrochemical interface. The GCE modified with COF-AuNPs was used as the working electrode. The immunosensor was fabricated by immobilizing a capture antibody through gold–amino affinity and incubating a secondary antibody via strong electrostatic interactions. It was reported that the LOD was as low as 2.00 fg/mL, enabling highly sensitive and selective detection with a short response time [20]. In the same year, Yin et al. introduced a label-free electrochemical immunosensor on the basis of PdPtCu@BP bilayer nanosheets (BNSs) for point-of-care (POC) testing of KIM-1. Benefiting from the excellent conductivity and peroxidase-mimicking activity of PdPtCu@BP BNSs, the sensor enabled rapid and sensitive label-free detection of KIM-1. It showed a linear range of 100 pg/mL–100 ng/mL with a minimum LOD of 32 pg/mL, making it suitable for POC applications [21].

3.4 | Application of a Biosensor for the Detection of KIM-1 in Real Urine Samples

Finally, the developed immunosensor was evaluated using real urine samples to assess its applicability for KIM-1 analysis. For this purpose, five different human urine samples were tested. As the presence of KIM-1 antigen in these samples was unknown, the standard addition method was applied to ensure accuracy. Initially, impedance measurements were recorded for each of the five urine samples without any KIM-1 antigen spiking. Subsequently, known concentrations of KIM-1 (10 and 50 fg/mL) were added to the same samples, and impedance measurements were repeated. Each measurement was performed in triplicate using separate biosensors to validate the reproducibility and reliability of the results. The corresponding KIM-1 concentrations were calculated using the calibration curve equation provided in Figure 4C ($y = 1571.2x + 10{,}981$). For each sample, the baseline KIM-1 level (prior to any addition) was recorded as the "[KIM-1] found by biosensor." After spiking with known concentrations of KIM-1, the new impedance responses were measured. Each spiked sample was analyzed in triplicate, and based on these results, the RSD values were calculated using the following equation:

$$\text{RSD\%} = (\text{Standard deviation} / \text{Mean value}) \times 100$$

Recovery referred to the ability of the biosensor to accurately detect and measure a known amount of analyte that had been intentionally added (spiked) into the real samples. The equation below was used for the calculation of recovery:

$$\text{Recovery (\%)} = (\text{Measured amount of KIM} - 1/ \text{Added amount of KIM} - 1) \times 100$$

The results of the applicability study for the KIM-1 biosensor using real urine samples are presented in Table 1. The typical detection range of KIM-1 antigen in standard ELISA assays is 150–10,000 pg/mL [2]. On the basis of the data provided in Table 1, it is clearly demonstrated that the developed KIM-1 immunosensor is capable of detecting KIM-1 levels in real urine samples with high sensitivity.

4 | Conclusion

Within the scope of this study, an electrochemical biosensor was developed by applying various surface modifications to a

TABLE 1 | Determination of kidney injury molecule-1 (KIM-1) levels in real urine samples with the designed biosensor.

Urine	[KIM-1] found by biosensor (fg/mL)	Standard added [KIM-1] (fg/mL)	Measured [KIM-1] by biosensor (fg/mL, $n = 3$)	RSD (%) ($n = 3$)	Recovery (%)
1	4.45	10	14.72/14.09/13.93	1.45	98.55
		50	53.57/55.51/54	0.165	99.84
2	3.32	10	13.96/13.06/14.07	2.77	102.77
		50	52.65/52.94/55.95	0.98	100.98
3	7.71	10	18.17/16.93/16.15	3.56	96.44
		50	56.78/58.41/56.15	1.04	98.96
4	1.91	10	11.98/11.22/11.57	2.69	97.31
		50	52.94/52.84/51.39	0.98	99.02
5	8.83	10	18.36/19.04/17.75	2.39	97.61
		50	58.83/58.25/57.75	0.95	99.05

Abbreviation: RSD, relative standard deviation.

QTF electrode, utilizing innovative strategies for the detection of KIM-1, a potential biomarker of AKI. Optimization studies were conducted for each step of the immobilization process, and optimal operational parameters were determined. Subsequently, comprehensive characterization studies—including repeatability, reproducibility, SFI, regeneration, specificity, and storage stability—were performed to validate the immunosensor's performance in terms of stability, selectivity, and reliability. To further support the characterization results, morphological changes on the immunosensor surface were investigated using AFM and SEM. The findings from all these studies demonstrated that the biosensor system developed for KIM-1 detection exhibits high stability and consistent performance. The designed KIM-1 immunosensor displayed a wide linear detection range (0.05–250 fg/mL), with low LOD (14.9 fg/mL) and LOQ (49.5 fg/mL). Additionally, the dissociation constant (K_d) for the antibody–antigen interaction was calculated as 148 ± 7 fg/mL, indicating strong binding affinity.

The developed immunosensor was successfully applied to real urine samples for KIM-1 detection. On the basis of the results obtained, it was concluded that the proposed immunosensor system holds strong potential for clinical application. Thanks to its QTF-based working electrode, practical fabrication method, fast response time, broad detection range, and reliable analytical performance, the KIM-1 immunosensor developed in this study represents a promising and advantageous platform for biomarker-based diagnostics.

Acknowledgments

The authors are grateful to the financial support from the Scientific and Technological Research Council of Çanakkale Onsekiz Mart University (FYL-2021-3807).

References

1. H. Abbiss, G. L. Maker, and R. D. Trengove, "Metabolomics Approaches for the Diagnosis and Understanding of Kidney Diseases," *Metabolites* 9, no. 2 (2019): 34.

2. R. N. Moresco, G. V. Bochi, C. S. Stein, J. A. De Carvalho, B. M. Cembranel, and Y. S. Bollick, "Urinary Kidney Injury Molecule-1 in Renal Disease," *Clinica Chimica Acta* 487 (2018): 15–21.

3. V. S. Vaidya, J. S. Ozer, F. Dieterle, et al., "Kidney Injury Molecule-1 Outperforms Traditional Biomarkers of Kidney Injury in Preclinical Biomarker Qualification Studies," *Nature Biotechnology* 28, no. 5 (2010): 478–485.

4. Z. Li, Z. Ju, and M. Frieri, "The T-Cell Immunoglobulin and Mucin Domain (Tim) Gene Family in Asthma, Allergy, and Autoimmunity," *Allergy and Asthma Proceedings* 34 (2013): e21–e26.

5. V. S. Vaidya, V. Ramirez, T. Ichimura, N. A. Bobadilla, and J. V. Bonventre, "Urinary Kidney Injury Molecule-1: A Sensitive Quantitative Biomarker for Early Detection of Kidney Tubular Injury," *American Journal of Physiology-Renal Physiology* 290, no. 2 (2006): F517–F529.

6. G. H. Tesch, "Serum and Urine Biomarkers of Kidney Disease: A Pathophysiological Perspective," *Nephrology* 15, no. 6 (2010): 609–616.

7. D. Kumar and D. Banerjee, "Methods of Albumin Estimation in Clinical Biochemistry: Past, Present, and Future," *Clinica Chimica Acta* 469 (2017): 150–160.

8. B. Jin, P. Wang, H. Mao, et al., "Multi-Nanomaterial Electrochemical Biosensor Based on Label-Free Graphene for Detecting Cancer Biomarkers," *Biosensors and Bioelectronics* 55 (2014): 464–469.

9. F. Arı, M. A. Ünal, M. K. Sezgintürk, and S. A. Özkan, "A Novel Electrochemical Approach to Biosensing Applications: Quartz Tuning Forks as Working Electrodes for Immunosensors," *Microchemical Journal* 195 (2023): 109484.

10. M. N. S. Karaboğa, M. A. Ünal, F. Arı, M. K. Sezgintürk, and S. A. Özkan, "An Innovative Method for the Detection of Alpha Synuclein, a Potential Biomarker of Parkinson's Disease: Quartz Tuning Fork-Based Mass Sensitive Immunosensor Design," *Physical Chemistry Chemical Physics* 26, no. 6 (2024): 5106–5114.

11. E. B. Aydın, M. Aydın, and M. K. Sezgintürk, "Determination of Calreticulin Using Fe_3O_4@AuNPs Core-Shell Functionalized With $PT(COOH)_2$ Polymer Modified Electrode: A New Platform for the Impedimetric Biosensing of Cancer Biomarkers," *Sensors and Actuators B: Chemical* 367 (2022): 132099.

12. M. Bilgi, M. Altun, M. Yılmaz, and M. K. Sezgintürk, "A Label-Free Immunosensor for the Simultaneous Electrochemical Determination of CA125 and HE4 Biomarkers for the Early Diagnosis of Ovarian Cancer," *Analytical and Bioanalytical Chemistry* 415 (2023): 1709–1718.

13. B. Özcan, B. Demirbakan, G. Yeşiller, and M. K. Sezgintürk, "Introducing a New Method for Evaluation of the Interaction Between an Antigen and an Antibody: Single Frequency Impedance Analysis for Biosensing Systems," *Talanta* 125 (2014): 7–13.

14. M. Mokni, A. Tlili, G. Attia, et al., "Novel Sensitive Immunosensor for the Selective Detection of Engrailed 2 Urinary Prostate Cancer Biomarker," *Biosensors and Bioelectronics* 217 (2022): 114678.

15. C. Özyurt, İ. Uludağ, and M. K. Sezgintürk, "An Ultrasensitive and Disposable Electrochemical Aptasensor for Prostate-Specific Antigen (PSA) Detection in Real Serum Samples," *Analytical and Bioanalytical Chemistry* 415 (2022): 1123–1136.

16. B. Demirbakan and M. K. Sezgintürk, "A Novel Ultrasensitive Immunosensor Based on Disposable Graphite Paper Electrodes for Troponin T Detection in Cardiovascular Disease," *Talanta* 213 (2020): 120779.

17. B. Özcan and M. K. Sezgintürk, "Graphene Oxide Based Electrochemical Label Free Immunosensor for Rapid and Highly Sensitive Determination of Tumor Marker HSP70," *Talanta* 160 (2016): 367–374.

18. H. Yang, H. Wang, C. Xiong, Y. Chai, and R. Yuan, "Highly Sensitive Electrochemiluminescence Immunosensor Based on ABEI/H_2O_2 System With PFO Dots as Enhancer for Detection of Kidney Injury Molecule-1," *Biosensors and Bioelectronics* 116 (2018): 16–22.

19. C. Liu, W. Yang, X. Min, et al., "An Enzyme-Free Electrochemical Immunosensor Based on Quaternary Metallic/Nonmetallic PdPtBP Alloy Mesoporous Nanoparticles/MXene and Conductive $CuCl_2$ Nanowires for Ultrasensitive Assay of Kidney Injury Molecule-1," *Sensors and Actuators B: Chemical* 334 (2021): 129585.

20. H. Boyacıoğlu, B. B. Yola, C. Karaman, O. Karaman, N. Atar, and M. L. Yola, "A Novel Electrochemical Kidney Injury Molecule-1 (KIM-1) Immunosensor Based Covalent Organic Frameworks-Gold Nanoparticles Composite and Porous $NiCo_2S_4$@CeO_2 Microspheres: The Monitoring of Acute Kidney Injury," *Applied Surface Science* 578 (2022): 152093.

21. Z. Yin, C. Liu, Y. Yi, H. Wu, X. Fu, and Y. Yan, "A Label-Free Electrochemical Immunosensor Based on PdPtCu@BP Bilayer Nanosheets for Point-of-Care Kidney Injury Molecule-1 Testing," *Journal of Electroanalytical Chemistry* 917 (2022): 116420.

Supporting Information

Additional supporting information can be found online in the Supporting Information section.

Supplementary Material: bab70128-sup-0001-SuppMat.docx